Environmental Science & Technology Letters

pubs.acs.org/journal/estlcu

Letter

Discrepancies between pH and Corrosive Indices of Hypersaline Effluents

Paz Nativ,* Gordon D. Z. Williams, and Avner Vengosh

Cite This: https://doi.org/10.1021/acs.estlett.5c01196

Read Online

ACCESS | Metrics & More | Article Recommendations | Supporting Information

ABSTRACT: Determining the pH of hypersaline wastewater is essential for regulatory compliance and the feasibility of geochemical and treatment processes. Hypersaline solutions have high ionic strength, which introduces deviations among measured proton activity, its concentration, and potential acidity. Here, we evaluate these deviations with theoretical simulations and by modeling hypersaline lithium brines from South America and produced waters from U.S. oil and gas operations (n > 60 000). We show that when the ionic strength increases above 2 m, proton activity coefficients steadily increase above unity. This causes the pH value to overestimate proton concentration. As this discrepancy increases, the pH alone cannot be used to accurately evaluate the solution's corrosivity by features such as the saturation index (SI) or calcium carbonate precipitation potential (CCPP). Our analysis reveals that 5% of the investigated produced waters showed pH values of <6 but positive CCPP or SI values, undermining pH as a single regulatory indicator of corrosivity. Accurate evaluation of hypersaline effluent corrosivity requires the utilization of advanced tools such as the PHREEQC software with the Pitzer model. This approach ensures a more reliable characterization of the potential hypersaline effluent corrosivity and thus more efficient management and policy.

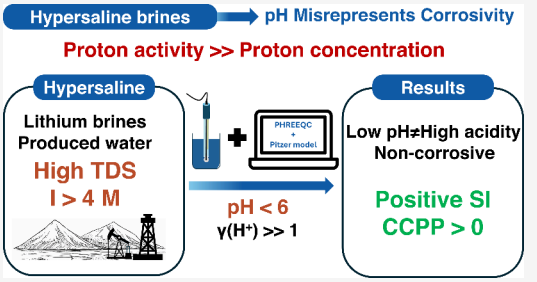

KEYWORDS: *pH, lithium, ionic strength, produced water, water management*

1. INTRODUCTION

Accurately measuring pH is one of the most important factors for understanding the geochemistry of natural waters, especially fluids with high salinity, such as lithium-rich brines or oil field-produced water. In the United States, the discharge of effluents must meet federal regulatory requirements, but permitting decisions are largely made at the state level.[1,2] U.S. EPA regulations require that the pH must be between 6 and 9 for potential ecological impacts upon the disposal of wastewater and mineral processing effluents.[3,4] This does not suggest that only the pH is important for regulations; a broad suite of parameters is also considered, including total dissolved solids (TDS), organic material, and specific toxins, among others. Likewise, pH is a critical factor for assessing the corrosivity of effluents from industrial process discharge on the environment.[5,6] However, in high-salinity water, accurately measuring pH (or proton activity) and interpreting its value are challenging due to complex ion interactions and large deviations from ideal conditions.

pH is a parameter of great importance for water analyses as it is crucial for assessing the acidity of natural waters, which directly influences the precipitation potential (PP) or saturation index (SI) for minerals, the assessment of the reduction−oxidation (RedOx) potential, and the saturation state of various gases.[7−10] The pH of a solution is defined as the negative base-10 logarithm of the activity of hydrogen ions (defined with round brackets (H^+)) in solution (pH = $-\log_{10}(H^+)$). In freshwaters, the activity of H^+ is approximately equal to the H^+ concentration (defined with square brackets, $[H^+]$); however, when the ionic strength (I, in molar (moles per liter) units "M" or molal unit (moles per kilogram weight) "m") or the TDS (in units of grams per liter) is high, H^+ activity cannot be approximated by its concentration, and the activity coefficient (γ) of protons must be used to calculate pH, as shown in eq 1:

$$\mathrm{pH} = -\log_{10}(\gamma_{H^+}[H^+]) \quad (1)$$

Under most natural water conditions, I is lower than ∼1−2 M (such as drinking water (I < 0.05 M), brackish water (I < 0.5 M), and seawater ($I \approx 0.7$ M)). As salinity increases, the activity coefficient of ions decreases below unity, and their activity (α) is lower than their concentrations (i.e., $\alpha_{H^+} < [H^+]$), mainly due to steric interference and ion pair interactions.[7,11] Under such conditions, ion activity can be calculated using the Davies[12] or Debye−Hückel extended

Received: December 1, 2025
Revised: December 28, 2025
Accepted: December 30, 2025

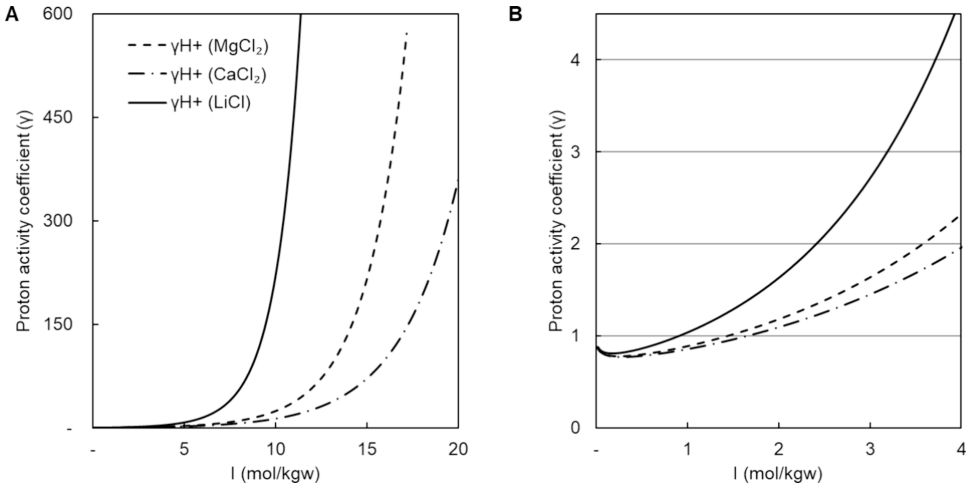

Figure 1. Simulations of the proton activity coefficient variations vs ionic strength (I) of solutions with three single-salt solutions ($MgCl_2$, $CaCl_2$, and LiCl) up to each salt solubility limit (5.73, 6.71, and 19.7 mol/kgw, respectively). Panel B provides a magnified view of the data shown in panel A (at I < 4 mol/kgw) for the sake of clarity.

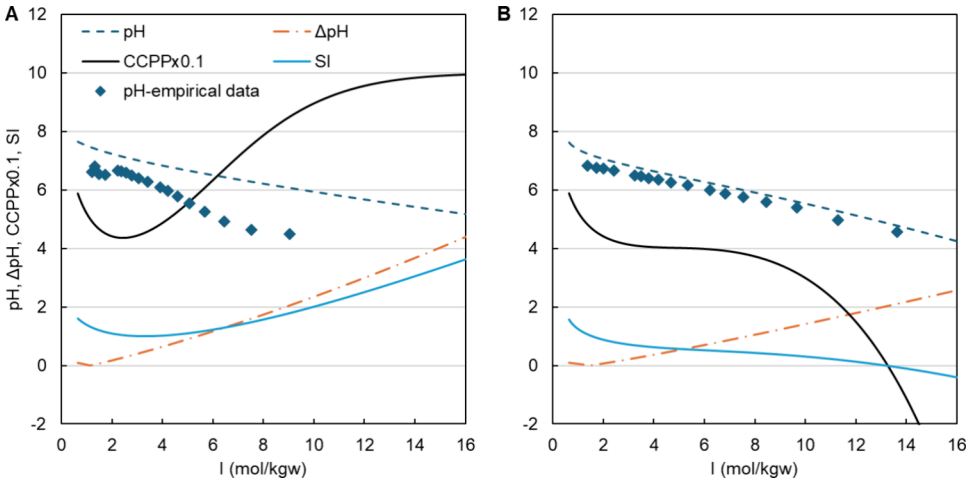

Figure 2. Empirically measured pH (discrete points) and PHREEQC simulation data of pH, ΔpH, SI, and CCPP values of calcite as a function of ionic strength, with two salt backgrounds: (A) LiCl and (B) $MgCl_2$ (baseline solution of 200 mM $CaCl_2$, alkalinity$_{(H_2CO_3^*)}$ of 2 mN, and initial pH of 7.66).

equation[13] (for I < 0.3 M), the specific ion interaction theory (SIT),[14] the Truesdell and Jones equation[15] (for I < 2 M), or a combination thereof.[9]

When I increases above 2 m, ion (and proton) activity coefficients may increase to values of more than 1, increasing the activity of ions above their concentration (i.e., $\alpha_{H^+} > [H^+]$), particularly for small and high-ionic potential ions (i.e., ions with a high charge-to-radius ratio such as H^+ or Mg^{2+}).[7,16−19] Under these conditions, the activity of water decreases below unity and the osmotic coefficient (a characterization of the solvent's deviation from ideal behavior) of water increases, reflecting the increasing deviation from ideal conditions. As a result, the ability of water to hydrate ions becomes limited, meaning that ions become more exposed and therefore more chemically reactive. This deviation directly influences the calculated activity coefficients of ions, as the osmotic coefficient is used to fit the empirical parameters in the Pitzer equations for ion activity calculations (see eqs S1 and S2 for more details).[19,20]

Under such high-salinity conditions (i.e., I > 2 m), the Pitzer approach is recognized as the reliable and accurate choice for evaluating ion interactions and calculating ion activities.[21−24] pH measurements using standard pH electrodes at low to moderate ionic strengths (I < 0.7 M) are well established and well developed, with accepted definitions and procedures.[21,24,25] However, pH measurements of hypersaline solutions require careful planning and understanding of several challenges. First, the change in the liquid junction potential (LJP) of the pH electrode[16,21,26−29] may cause a shift in the analytical readings, typically toward lower pH values (or more accurately, higher electrical potential readings). Second, due to the high activity coefficient of protons, the pH calculated from the activity of H^+ may deviate from the actual concentration of H^+ by orders of magnitude, as demonstrated in this study (Figures 1 and 2).[16−18]

Here, we investigate how pH deviates from H^+ concentration at increased salinity ($I \approx$ 2−15 m), which has important implications for corrosivity assessment and regulatory frameworks of hypersaline brines. We investigated reported data from more than 60 000 hypersaline brines, including closed-basin lithium-rich brines from the Lithium Triangle in South America, as well as oil and gas formation/

https://doi.org/10.1021/acs.estlett.5c01196
Environ. Sci. Technol. Lett. XXXX, XXX, XXX−XXX

produced waters from the United States. We show that more than 5% of the analyzed brines were not corrosive to calcite, despite their pH values being less than 6 and therefore classified as acidic solutions.[3,4] This study has important implications for environmental regulations and process designs, including direct lithium extraction (DLE) and CO_2 injection for carbon storage in aquifers composed of hypersaline solutions. Using the study findings will help to better determine the acidity potential of hypersaline solutions with complex chemistry, especially where pH measurements alone are insufficient.

2. MATERIALS AND METHODS

2.1. Natural Brines and Hypersaline Effluent Data

This study includes analyses of (1) lithium-rich closed-basin brines, both natural and from evaporation ponds from the Lithium Triangle in South America (n = 552; no alkalinity data are present),[6,30−55] and (2) produced waters, from the USGS produced waters geochemical database, including brines classified by the USGS as coal bed methane (CBM), geothermal, shale, sedimentary, and injection that are common wastewaters derived from oil and natural gas operations in the United States (n = 61 222). For all produced water, only sources with complete chemistry data on major ions and alkalinity, pH, and density values were considered from the USGS full data set (n_{total} = 113 136).[56]

2.2. Software and Simulations

All characterizations and simulations were performed with the PHREEQC interactive software (version 3.7.3315968)[9] using the Pitzer database.[20]

2.3. Parameters

ΔpH was defined to represent the absolute difference between the pH calculated by using the activity of H^+ ((H^+)) and the actual concentration of H^+ ($[H^+]$) of a solution (eq 2).

$$\Delta pH = |p(H^+) - p[H^+]| \quad (2)$$

2.4. pH Measurement Setup

For pH measurements, a Metrohm combined pH glass electrode (3 M KCl) was used with a Metrohm ECO Titrator as the controller at Duke University. The temperature was measured manually. All chemicals used were of analytical grade and dried at 50 °C before use. A method for more accurate pH determination in hypersaline solutions is proposed for this study (see below).

3. RESULTS AND DISCUSSION

3.1. Theoretical Evaluation of Hypersaline Fluids

We evaluate the effect of salinity and different chemical compositions of fluids (e.g., pure $MgCl_2$, $CaCl_2$, and LiCl) on the variations of the H^+ activity coefficient across a range of ionic strengths from 0 to 20 m. Panels A and B of Figure 1 present the calculated proton activity coefficient as a function of the ionic strength of the different saline solutions, showing the initial decrease in the activity coefficient with an increase in ionic strength, mainly due to steric interference[7,11] (Figure 1B), and a steady increase above unity with an increase in salinity (I > 2 m), with proton activity coefficient values reaching ∼150 at I > 10 m (Figure 1A).

Calcite ($CaCO_3$) is a common mineral with pH-dependent solubility, typically dissolving under acidic conditions, and its solubility is used as a reference for regulatory applications.[3,4,57] One can examine calcite solubility using two different approaches of calculations: (1) saturation index (SI), calculated by reducing the $CaCO_3$ equilibrium constant (K_{sp}) from the ion activity product (IAP) of the solubility equation, in a log function, as shown in eq 4, and (2) calcium carbonate precipitation potential (CCPP), calculated quantitatively in step iterations and defined as the mass of calcite required to reach $Q = K'_{sp}$, where Q is the product of the ion's concentrations in eq 3 and K'_{sp} is the apparent solubility constant of calcite.[7,11]

$$CaCO_{3(s)} \rightleftharpoons Ca^{2+} + CO_3^{2-};\ K_{sp} = 10^{-8.48} \quad (3)$$

$$SI = \log_{10}\left(\frac{IAP}{K_{sp}}\right) \quad (4)$$

To test the extent of the phenomenon, we conducted lab experiments in which a synthetic solution (200 mM $CaCl_2$, $alkalinity_{(H_2CO_3^*)}$ of 2 mN, an initial pH of 7.66, and SI and CCPP (milligrams per liter as $CaCO_3$) values for calcite of 1.61 and 58.77, respectively) was used as the baseline. $MgCl_2$ and LiCl solutions were added to this baseline solution to increase the ionic strength, and the solution pH was measured empirically. Using PHREEQC, the pH, ΔpH (i.e., the difference between the measured pH and the real proton concentration), calcite SI, and CCPP values were calculated for both experiments. The simulated and empirical results are presented in Figure 2. The results show that the calculated pH of all simulations decreases below 6 at high ionic strengths (I > 8−10 m), a pH at which calcite is typically considered to be dissolved (or undersaturated). However, the ionic composition has a significant impact on the tested saturation indices of calcite. The addition of lithium ions increases ionic strength and decreases the pH, but due to a low level of ionic complexation with carbonate ions or hydroxide, SI and CCPP remain positive (Figure 2A), meaning that the solution remains supersaturated with calcite even at pH values of less than 6. In contrast, the addition of magnesium ions (Figure 2B) forms ion complexes with both hydroxide and carbonate ions, thus reducing the available carbonate ion concentration. Therefore, the SI and CCPP values decrease below zero, meaning that calcite became undersaturated (corrosive) at pH <6. In both scenarios, the ΔpH parameter increases with I, reflecting the discrepancy of the measured pH from the proton concentration. Notably, the measured pH is lower than the calculated pH (Figure 2A); such variations are well-known and result from inaccuracies in the standard pH measurement.[21,26,26,28]

For accurate pH determination in saline solutions, we recommend the methods presented in refs 21 and 26. However, these methods are less suitable when the ionic strength exceeds 6 m or when divalent ions occur at high concentrations. For example, the chloride ion-selective electrodes used in ref 26 for pH calibration and verification are not suitable for ionic strengths above 1 m and may produce unstable readings in high-salinity solutions.[58,59] Using custom pH buffer solutions, as suggested by refs 21 and 60, under such high-salinity conditions requires the Pitzer model to simulate the buffer solution pH, as the SIT model, which is broader and contains abundant weak acid and ion data, is not applicable. On the other hand, the addition of weak acid systems required to produce a pH buffer solution to the Pitzer database is applicable only in solutions without high divalent ion concentrations, due to a lack of literature data.[61] Hence, a new method for pH calibration is required, using a custom pH

https://doi.org/10.1021/acs.estlett.5c01196
Environ. Sci. Technol. Lett. XXXX, XXX, XXX−XXX

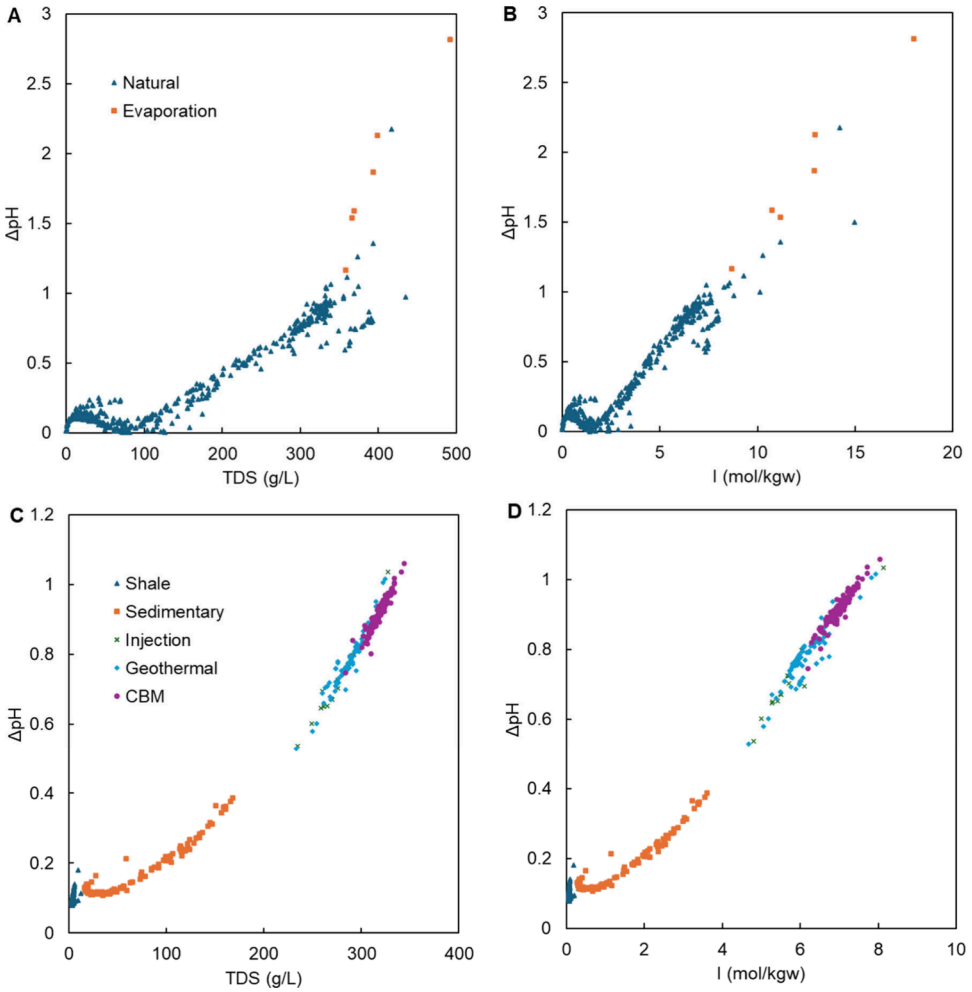

Figure 3. Calculated ΔpH value as a function of the effluents' TDS and ionic strength. (A and B) Lithium brine effluents from natural and evaporation ponds (n = 552).[6,30−55] (C and D) USGS produced waters geochemical database, with the sources of hydrocarbon mining types being coal (coal bed methane (CBM)-produced water), geothermal, shale, sedimentary, and injection (n = 61 222; the data were averaged and grouped to reduce overplotting, the data were grouped into bins of I, and values were averaged arithmetically[56]).

buffer solution simulated with an unmodified Pitzer model to accurately measure pH in hypersaline solutions with I > 6 m. This method is currently being developed by the authors but is beyond the scope of this study.

Based on this theoretical assessment and the experiments we conducted, the following conclusions can be deduced. (i) The ionic composition of a brine or wastewater has a significant role in the osmotic and activity coefficient, and this effect may not be linear or conservative and therefore varies among different brine types with different chemistry (e.g., lithium-rich vs magnesium-rich brines). (ii) Proton activity alone cannot serve as an estimate of proton concentration in high-salinity brines or in a complex ionic matrix. (iii) When proton activity differs by orders of magnitude from its concentration, corrosivity calculations must be carefully considered for avoiding the mismatch between pH and potential corrosivity.

3.2. Natural Brines and Hypersaline Effluent Data

We used published water chemistry data of different hypersaline brines and effluents to evaluate the role of salinity and ion composition on their ΔpH values and the potential discrepancy between measured pH and potential corrosivity. This evaluation aims to test if natural brines and produced waters (i.e., real-life scenarios) exhibit the same trends shown in the experimental synthetic solutions (Figure 2). Many of the brines used in the simulation and calculations are considered wastewater or effluent and are therefore regulated accordingly. The first set of data are closed-basin lithium-rich brines, both natural and from evaporation ponds from locations throughout the world (Figure 3A,B; n = 552).[6,30−55] The second set consists of produced waters from the large USGS produced waters geochemical database, including brines classified by the USGS as coal bed methane (CBM), geothermal, shale, sedimentary, and injection that are typical wastewaters derived from oil and natural gas operations in the United States (Figure 3C,D; n = 61 222).[56]

The results show an almost linear trend between an increasing ionic strength and ΔpH (Figure 3 B,D) for the whole range of brine salinities. The results show that the ΔpH values disperse at high TDS values (>350 g/L) of some of the lithium-rich brines, likely due to the extremely high salinity. Regardless, the trend is the same, the ΔpH increasing with salinity.

ΔpH allows us to assess the magnitude of the difference between the measured pH and the actual available protons for reactions (i.e., acidity potential), as this difference is crucial for the calculation of water quality parameters such as CCPP or corrosivity. CCPP was calculated for all of the produced waters

https://doi.org/10.1021/acs.estlett.5c01196
Environ. Sci. Technol. Lett. XXXX, XXX, XXX−XXX

at pH <6, and positive CCPP values were filtered out; 3035 effluents met these criteria (~5% of the data set of 61 222), with average TDS and ΔpH values of 290.5 g/L and 0.82, respectively. This test shows that a large discrepancy exists between the proton activity and concentration in brines with moderate to high salinity, enabling positive CCPP values even under relatively (apparent) acidic conditions (pH <6), which is commonly the regulatory limit.[3,4] This means that despite a low pH, the potential negative effects (i.e., corrosivity) associated with these low-pH brines (some of which can be considered wastewaters) do not apply at high salinity. This high ΔpH and positive CCPP discrepancy are primarily found in the CBM, geothermal, and injection brines, accounting for 95% of all of the identified discrepancies (Figure 3C).

Overall, this study demonstrates that in high-salinity solutions the measured pH does not reliably reflect the true chemical conditions of the solution. A high ionic strength or TDS leads to increased proton activity coefficients, resulting in low pH values that do not necessarily indicate higher proton concentrations and thus corrosivity or undersaturation with respect to soluble minerals, such as calcite. These deviations are nonlinear, and different parameters depend on the chemical composition of the solution, making the task of characterizing a hypersaline brine highly specific with few general rules of thumb. Our results show that the underlying chemical composition plays a crucial role in controlling the proton activity coefficients and saturation indices, with significant implications for the calculation of water quality parameters such as SI and CCPP.

These results suggest that relying solely on pH for regulatory compliance and engineering operations for hypersaline effluents may result in erroneous estimations of the potential corrosivity. Although EPA guidelines set the pH range to be between 6 and 9 and permits of the state level consider a broad, multiparameter criteria for each case, pH remains a significant indicator of corrosivity risk. For example, the carbon capture process of injecting CO_2 into deep saline aquifers is directly related to the ability of the saline solution to adsorb the CO_2 gas, which is a pH-dependent process. In addition, Williams et al.[5,6] reported that both natural and evaporation lithium ponds had pH values ranging from 7.09 to 3.18, with all sources having negative SI values (corrosive to calcite), emphasizing the need for comprehensive brine characterization. The chemical composition of the water source is critical; for example, high calcium concentrations may induce a positive SI or CCPP value, even at very low pH values. Therefore, when using the measured pH value as a sole regulatory indicator, unnecessary effluent treatment may be performed to meet regulatory requirements, which in turn can lead to excess costs or even future project cancellations. For better evaluation of effluent corrosivity or accurate chemical characteristics, more advanced tools must be used, such as the PHREEQC simulation software with the Pitzer database and a suitable pH measuring technique for hypersaline solutions. Also, standard simulation tools such as the Water-TAP3 software[62] should be updated to include more detailed analysis options for hypersaline solutions, such as ΔpH, which is developed in this Letter. This manner of operation ensures more reliable water characterization, which, in turn, leads to more efficient decision-making.

■ ASSOCIATED CONTENT

Supporting Information

The Supporting Information is available free of charge at https://pubs.acs.org/doi/10.1021/acs.estlett.5c01196.

Osmotic coefficient, with respect to water activity, ionic strength, and chemical composition, and cation activity coefficient calculations, as developed by the Pitzer approach, are described in eqs S1 and S2, respectively (PDF)

■ AUTHOR INFORMATION

Corresponding Author

Paz Nativ − *Division of Earth and Climate Sciences, Nicholas School of the Environment, Duke University, Durham, North Carolina 27708, United States;* orcid.org/0000-0002-0849-4880; Email: paznativ@gmail.com

Authors

Gordon D. Z. Williams − *Division of Earth and Climate Sciences, Nicholas School of the Environment, Duke University, Durham, North Carolina 27708, United States;* orcid.org/0000-0002-9076-9635

Avner Vengosh − *Division of Earth and Climate Sciences, Nicholas School of the Environment, Duke University, Durham, North Carolina 27708, United States;* orcid.org/0000-0001-8928-0157

Complete contact information is available at: https://pubs.acs.org/10.1021/acs.estlett.5c01196

Notes

The authors declare no competing financial interest.

■ ACKNOWLEDGMENTS

This study was supported by the Duke University Climate Research Innovation Seed Program, CRISP, the Duke University Josiah Charles Trent Memorial Foundation Endowment Fund, and the Critical Minerals Hub at Duke University.

■ REFERENCES

(1) McLaughlin, M. C.; Borch, T.; McDevitt, B.; Warner, N. R.; Blotevogel, J. Water Quality Assessment Downstream of Oil and Gas Produced Water Discharges Intended for Beneficial Reuse in Arid Regions. *Science of The Total Environment* **2020**, *713*, 136607.

(2) Cooper, C. M.; McCall, J.; Stokes, S. C.; McKay, C.; Bentley, M. J.; Rosenblum, J. S.; Blewett, T. A.; Huang, Z.; Miara, A.; Talmadge, M.; Evans, A.; Sitterley, K. A.; Kurup, P.; Stokes-Draut, J. R.; Macknick, J.; Borch, T.; Cath, T. Y.; Katz, L. E. Oil and Gas Produced Water Reuse: Opportunities, Treatment Needs, and Challenges. *ACS EST Eng.* **2022**, *2* (3), 347−366.

(3) 40 CFR Part 436 -- Mineral Mining and Processing Point Source Category. https://www.ecfr.gov/current/title-40/part-436 (accessed 2025-05-16).

(4) 40 CFR Part 440 -- Ore Mining and Dressing Point Source Category. https://www.ecfr.gov/current/title-40/part-440 (accessed 2025-05-16).

(5) Williams, G. D. Z.; Vengosh, A. Quality of Wastewater from Lithium-Brine Mining. *Environ. Sci. Technol. Lett.* **2025**, *12* (2), 151−157.

(6) Williams, G. D. Z.; Nativ, P.; Vengosh, A. The Role of Boron in Controlling the pH of Lithium Brines. *Sci. Adv.* **2025**, *11* (21), No. eadw3268.

(7) Benjamin, M. M. *Water Chemistry*; McGraw-Hill: New York, 2002.

(8) Birnhack, L.; Lahav, O. *Post-Treatment of Desalinated Water-Chemistry, Design, Engineering, and Implementation*; Elsevier Inc., 2018.
(9) Charlton, S. R.; Parkhurst, D. L. Modules Based on the Geochemical Model PHREEQC for Use in Scripting and Programming Languages. *Computers & Geosciences* **2011**, *37* (10), 1653−1663.
(10) Tchobanoglous, G.; Burton, F. L.; Tsuchihashi, R. *Wastewater Engineering: Treatment and Resource Recovery*; McGraw-Hill Professional: New York, 2014.
(11) Lahav, O.; Birnhack, L. *Aquatic Chemistry*; De Gruyter: Berlin, 2019.
(12) Davies, C. W., 397 The Extent of Dissociation of Salts in Water. Part VIII. An Equation for the Mean Ionic Activity Coefficient of an Electrolyte in Water, and a Revision of the Dissociation Constants of Some Sulphates. *J. Chem. Soc.* **1938**, No. 0, 2093−2098.
(13) Debye, P.; Hückel, E. The Theory of Electrolytes. I. Lowering of Freezing Point and Related Phenomena. *Phys. Z.* **1923**, No. 24, 185−206.
(14) Sipos, P. Application of the Specific Ion Interaction Theory (SIT) for the Ionic Products of Aqueous Electrolyte Solutions of Very High Concentrations. *J. Mol. Liq.* **2008**, *143* (1), 13−16.
(15) Truesdell, A. H.; Jones, B. F. WATEQ, a Computer Program for Calculating Chemical Equilibria of Natural Waters. *J. Res. U.S. Geol. Surv.* **1974**, *2* (2), 233−248.
(16) Degoulange, D.; Dubouis, N.; Grimaud, A. Toward the Understanding of Water-in-Salt Electrolytes: Individual Ion Activities and Liquid Junction Potentials in Highly Concentrated Aqueous Solutions. *J. Chem. Phys.* **2021**, *155* (6), 064701.
(17) Zhang, L.; Zhang, C.; Berg, E. J. Mastering Proton Activities in Aqueous Batteries. *Adv. Mater.* **2025**, DOI: 10.1002/adma.202407852.
(18) Van Hees, A.; Zhang, C. Electrostatic Aspect of the Proton Reactivity in Concentrated Electrolyte Solutions. *J. Phys. Chem. Lett.* **2024**, *15* (49), 12212−12217.
(19) Pitzer, K. S. *Activity Coefficients in Electrolyte Solutions*, 2nd ed.; CRC Press: Boca Raton, FL, 2018.
(20) Pitzer, K. S. Thermodynamics of Electrolytes. I. Theoretical Basis and General Equations. *J. Phys. Chem.* **1973**, *77* (2), 268−277.
(21) Nir, O.; Marvin, E.; Lahav, O. Accurate and Self-Consistent Procedure for Determining pH in Seawater Desalination Brines and Its Manifestation in Reverse Osmosis Modeling. *Water Res.* **2014**, *64*, 187−195.
(22) Millero, F. J. Use of the Pitzer Equations to Examine the Dissociation of TRIS in NaCl Solutions. *J. Chem. Eng. Data* **2009**, *54* (2), 342−344.
(23) Ferra, M. I. A.; Graça, J. R.; Marques, A. M. M. Application of the Pitzer Model to Assignment of pH to Phthalate Standard Buffer Solutions. *J. Solution Chem.* **2009**, *38* (11), 1433−1448.
(24) Marion, G. M.; Millero, F. J.; Camões, M. F.; Spitzer, P.; Feistel, R.; Chen, C.-T. A. pH of Seawater. *Marine Chemistry* **2011**, *126* (1), 89−96.
(25) Buck, R. P.; Rondinini, S.; Covington, A. K.; Baucke, F. G. K.; Brett, C. M. A.; Camoes, M. F.; Milton, M. J. T.; Mussini, T.; Naumann, R.; Pratt, K. W.; Spitzer, P.; Wilson, G. S. Measurement of pH. Definition, Standards, and Procedures (IUPAC Recommendations 2002). *Pure Appl. Chem.* **2002**, *74* (11), 2169−2200.
(26) Golan, R.; Gavrieli, I.; Lazar, B.; Ganor, J. The Determination of pH in Hypersaline Lakes with a Conventional Combination Glass Electrode. *Limnology and Oceanography: Methods* **2014**, *12* (11), 810−815.
(27) Ben-Yaakov, S.; Sass, E. Independent Estimate of the pH of Dead Sea Brine. *Limnology and Oceanography* **1977**, *22* (2), 374−376.
(28) Marcus, Y. Determination of pH in Highly Saline Waters. *Pure Appl. Chem.* **1989**, *61* (6), 1133−1138.
(29) Knauss, K. G.; Wolery, T. J.; Jackson, K. J. A New Approach to Measuring pH in Brines and Other Concentrated Electrolytes. *Geochim. Cosmochim. Acta* **1990**, *54* (5), 1519−1523.
(30) Garrett, D. E. Part 1 - Lithium. In *Handbook of Lithium and Natural Calcium Chloride*; Garrett, D. E., Ed.; Academic Press: Oxford, U.K., 2004; pp 1−235.
(31) Risacher, F.; Fritz, B. Geochemistry of Bolivian Salars, Lipez, Southern Altiplano: Origin of Solutes and Brine Evolution. *Geochim. Cosmochim. Acta* **1991**, *55* (3), 687−705.
(32) Lucrecia López Steinmetz, R.; Salvi, S.; Gabriela García, M.; Peralta Arnold, Y.; Béziat, D.; Franco, G.; Constantini, O.; Córdoba, F. E.; Caffe, P. J. Northern Puna Plateau-Scale Survey of Li Brine-Type Deposits in the Andes of NW Argentina. *J. Geochem. Explor.* **2018**, *190*, 26−38.
(33) López Steinmetz, R. L.; Salvi, S.; Sarchi, C.; Santamans, C.; López Steinmetz, L. C. Lithium and Brine Geochemistry in the Salars of the Southern Puna, Andean Plateau of Argentina. *Economic Geology* **2020**, *115* (5), 1079−1096.
(34) Garcia, M. G.; Borda, L. G.; Godfrey, L. V.; López Steinmetz, R. L.; Losada-Calderon, A. Characterization of Lithium Cycling in the Salar De Olaroz, Central Andes, Using a Geochemical and Isotopic Approach. *Chem. Geol.* **2020**, *531*, 119340.
(35) Borda, L. G.; Godfrey, L. V.; Del Bono, D. A.; Blanco, C.; García, M. G. Low-Temperature Geochemistry of B in a Hypersaline Basin of Central Andes: Insights from Mineralogy and Isotopic Analysis (δ^{11}B and ^{87}Sr/^{86}Sr). *Chem. Geol.* **2023**, *635*, 121620.
(36) Pueyo, J. J.; Chong, G.; Ayora, C. Lithium Saltworks of the Salar de Atacama: A Model for MgSO4-Free Ancient Potash Deposits. *Chem. Geol.* **2017**, *466*, 173−186.
(37) Meixner, A.; Alonso, R. N.; Lucassen, F.; Korte, L.; Kasemann, S. A. Lithium and Sr Isotopic Composition of Salar Deposits in the Central Andes across Space and Time: The Salar de Pozuelos, Argentina. *Miner Deposita* **2022**, *57* (2), 255−278.
(38) Sarchi, C.; Lucassen, F.; Meixner, A.; Caffe, P. J.; Becchio, R.; Kasemann, S. A. Lithium Enrichment in the Salar de Diablillos, Argentina, and the Influence of Cenozoic Volcanism in a Basin Dominated by Paleozoic Basement. *Miner Deposita* **2023**, *58* (7), 1351−1370.
(39) Álvarez-Amado, F.; Tardani, D.; Poblete-González, C.; Godfrey, L.; Matte-Estrada, D. Hydrogeochemical Processes Controlling the Water Composition in a Hyperarid Environment: New Insights from Li, B, and Sr Isotopes in the Salar de Atacama. *Science of The Total Environment* **2022**, *835*, 155470.
(40) Godfrey, L. V.; Chan, L.-H.; Alonso, R. N.; Lowenstein, T. K.; McDonough, W. F.; Houston, J.; Li, J.; Bobst, A.; Jordan, T. E. The Role of Climate in the Accumulation of Lithium-Rich Brine in the Central Andes. *Appl. Geochem.* **2013**, *38*, 92−102.
(41) Vengosh, A.; Chivas, A. R.; Starinsky, A.; Kolodny, Y.; Baozhen, Z.; Pengxi, Z. Chemical and Boron Isotope Compositions of Non-Marine Brines from the Qaidam Basin, Qinghai, China. *Chem. Geol.* **1995**, *120* (1), 135−154.
(42) Sieland, R.; Schmidt, N.; Schön, A.; Schreckenbach, J.; Merkel, B. *Geochemische, Hydrogeologische Und Feinstratigraphische Untersuchungen Am. Salar de Uyuni (Bolivien)*; TU Bergakademie: Freiberg, Germany, 2011.
(43) Haferburg, G.; Gröning, J. A. D.; Schmidt, N.; Kummer, N.-A.; Erquicia, J. C.; Schlömann, M. Microbial Diversity of the Hypersaline and Lithium-Rich Salar de Uyuni, Bolivia. *Microbiological Research* **2017**, *199*, 19−28.
(44) Zheng, M.; Liu, X. Hydrochemistry of Salt Lakes of the Qinghai-Tibet Plateau, China. *Aquat Geochem* **2009**, *15* (1), 293−320.
(45) Rettig, S. L.; Jones, B. F.; Risacher, F. Geochemical Evolution of Brines in the Salar of Uyuni, Bolivia. *Chem. Geol.* **1980**, *30*, 57−79.
(46) Shi, Z.; Tan, H.; Xue, F.; Li, Y.; Zhang, X.; Cong, P.; Santosh, M.; Zhang, Y. Hydrochemical Evolution and Source Mechanisms Governing the Unusual Lithium and Boron Enrichment in Salt Lakes of Northern Tibet. *GSA Bulletin* **2024**, *136*, 5174.
(47) *cochilco; sernageomin. Compilación de Informes Sobre Mercado Internacional Del Litio y Potencial Del Litio En Salares Del Norte de Chile*; Secretaría de Minería: Santiago, 2013.https://www.cochilco.cl/web/download/362/2013/7111/compilacion-de-informes-sobre-mercado-internacional-del-litio-y-el-potencial-de-litio-en-salares-del-norte-de-chile.pdf.

https://doi.org/10.1021/acs.estlett.5c01196
Environ. Sci. Technol. Lett. XXXX, XXX, XXX−XXX

(48) Vignoni, P. A.; Jurikova, H.; Schröder, B.; Tjallingii, R.; Córdoba, F. E.; Lecomte, K. L.; Pinkerneil, S.; Grudzinska, I.; Schleicher, A. M.; Viotto, S. A.; Santamans, C. D.; Rae, J. W. B.; Brauer, A. On the Origin and Processes Controlling the Elemental and Isotopic Composition of Carbonates in Hypersaline Andean Lakes. *Geochim. Cosmochim. Acta* **2024**, *366*, 65−83.
(49) Muller, E.; Gaucher, E. C.; Durlet, C.; Moquet, J. S.; Moreira, M.; Rouchon, V.; Louvat, P.; Bardoux, G.; Noirez, S.; Bougeault, C.; Vennin, E.; Gérard, E.; Chavez, M.; Virgone, A.; Ader, M. The Origin of Continental Carbonates in Andean Salars: A Multi-Tracer Geochemical Approach in Laguna Pastos Grandes (Bolivia). *Geochim. Cosmochim. Acta* **2020**, *279*, 220−237.
(50) Davis, J. R. Late Cenozoic Geology of Clayton Valley, Nevada and the Genesis of a Lithium-Enriched Brine. Ph.D. Thesis, The University of Texas at Austin, Austin, TX, 1981. https://www.proquest.com/docview/303206494?fromopenview=true&pq-origsite=gscholar&sourcetype=Dissertations%20&%20Theses.
(51) Risacher, F.; Alonso, H.; Salazar, C. *Geoquímica En Cuencas Cerradas: I, II y III*; Convenio de Cooperación DGA-UCN-Orstom: Santiago, 1999; Vol. *51*. https://app.ingemmet.gob.pe/biblioteca/pdf/Geoq-5.pdf.
(52) Smith, G. I.; Stuiver, M. Subsurface Stratigraphy and Geochemistry of Late Quaternary Evaporites, Searles Lake, California, with a Section on Radiocarbon Ages of Stratigraphic Units. Technical Report 1043; U.S. Government Printing Office: Washington, DC, 1979.
(53) Godfrey, L.; Álvarez-Amado, F. Volcanic and Saline Lithium Inputs to the Salar de Atacama. *Minerals* **2020**, *10* (2), 201.
(54) López Steinmetz, R. L. Lithium- and Boron-Bearing Brines in the Central Andes: Exploring Hydrofacies on the Eastern Puna Plateau between 23° and 23°30′S. *Miner Deposita* **2017**, *52* (1), 35−50.
(55) Zhang, W.; Tan, H.; Xu, W.; Huang, J. Boron Source and Evolution of the Zabuye Salt Lake, Tibet: Indication from Boron Geochemistry and Isotope. *Appl. Geochem.* **2023**, *148*, 105516.
(56) Blondes, M. S.; Knierim, K. J.; Croke, M. R.; Freeman, P. A.; Doolan, C.; Herzberg, A. S.; Shelton, J. L. *U.S. Geological Survey National Produced Waters Geochemical Database*, ver. 3.0; 2023.
(57) Lahav, O.; Birnhack, L. Quality Criteria for Desalinated Water Following Post-Treatment. *Desalination* **2007**, *207* (1−3), 286−303.
(58) Gonski, S. F.; Luther, G. W.; Kelley, A. L.; Martz, T. R.; Roberts, E. G.; Li, X.; Dong, B.; Watson, J. A.; Wirth, T. S.; Hussain, N.; Feris Serrano, R. J.; Hale, E.; Cai, W.-J. A Half-Cell Reaction Approach for pH Calculation Using a Solid-State Chloride Ion-Selective Electrode with a Hydrogen Ion-Selective Ion-Sensitive Field Effect Transistor. *Marine Chemistry* **2024**, *261*, 104373.
(59) Takeshita, Y.; Martz, T. R.; Johnson, K. S.; Dickson, A. G. Characterization of an Ion Sensitive Field Effect Transistor and Chloride Ion Selective Electrodes for pH Measurements in Seawater. *Anal. Chem.* **2014**, *86* (22), 11189−11195.
(60) Dagan-Jaldety, C.; Lahav, O.; Ben-Asher, R.; Saller, G.; Oz, S.; Nativ, P. Innovative Ammonia Harvesting from Wastewater: A Controlled Closed-Loop Process at High pH for Enhanced Nutrient Recovery. *Chemical Engineering Journal* **2025**, *503*, 158201.
(61) Moog, H. C.; Bok, F.; Marquardt, C. M.; Brendler, V. Disposal of Nuclear Waste in Host Rock Formations Featuring High-Saline Solutions − Implementation of a Thermodynamic Reference Database (THEREDA). *Appl. Geochem.* **2015**, *55*, 72−84.
(62) *Water-TAP3: Water Technoeconomic Assessment Pipe-Parity Platform*. https://www.nawihub.org/water-tap3/ (accessed 2025-11-26).

https://doi.org/10.1021/acs.estlett.5c01196
Environ. Sci. Technol. Lett. XXXX, XXX, XXX−XXX